

CANCER

The androgen receptor regulates a druggable translational regulon in advanced prostate cancer

Yuzhen Liu^{1*}, Jessie L. Horn^{1*}, Kalyan Banda^{1*}, Asha Z. Goodman¹, Yiting Lim¹, Sujata Jana¹, Sonali Arora¹, Alexandre A. Germanos¹, Lexiaochuan Wen¹, William R. Hardin¹, Yu C. Yang¹, Ilsa M. Coleman¹, Robin G. Tharakan¹, Elise Y. Cai¹, Takuma Uo², Smitha P. S. Pillai³, Eva Corey⁴, Colm Morrissey⁴, Yu Chen⁵, Brett S. Carver⁶, Stephen R. Plymate², Slobodan Beronja¹, Peter S. Nelson^{1,7}, Andrew C. Hsieh^{1,7†}

Copyright © 2019
The Authors, some
rights reserved;
exclusive licensee
American Association
for the Advancement
of Science. No claim
to original U.S.
Government Works

The androgen receptor (AR) is a driver of cellular differentiation and prostate cancer development. An extensive body of work has linked these normal and aberrant cellular processes to mRNA transcription; however, the extent to which AR regulates posttranscriptional gene regulation remains unknown. Here, we demonstrate that AR uses the translation machinery to shape the cellular proteome. We show that AR is a negative regulator of protein synthesis and identify an unexpected relationship between AR and the process of translation initiation *in vivo*. This is mediated through direct transcriptional control of the translation inhibitor 4EBP1. We demonstrate that lowering AR abundance increases the assembly of the eIF4F translation initiation complex, which drives enhanced tumor cell proliferation. Furthermore, we uncover a network of pro-proliferation mRNAs characterized by a guanine-rich cis-regulatory element that is particularly sensitive to eIF4F hyperactivity. Using both genetic and pharmacologic methods, we demonstrate that dissociation of the eIF4F complex reverses the proliferation program, resulting in decreased tumor growth and improved survival in preclinical models. Our findings reveal a druggable nexus that functionally links the processes of mRNA transcription and translation initiation in an emerging class of lethal AR-deficient prostate cancer.

INTRODUCTION

The androgen receptor (AR) is a nuclear hormone receptor that is activated by androgens to promote its function as a transcription factor (1). Specificity is mediated in part through receptor recognition of a palindromic dihexameric DNA motif called the androgen response element (ARE), which controls gene expression through recruitment of coactivators or corepressors (2). Although the role of AR in regulating transcription is well established, it is unknown whether AR uses additional processes such as translation control to direct protein abundance and cellular phenotypes. This is a particularly timely question because translation regulation is emerging as a critical determinant of proteome diversity, tissue homeostasis, and disease (3–5).

One disease that has demonstrated sensitivity to inhibition of AR and mRNA translation is prostate cancer. Ninety percent of early-stage human prostate cancers are dependent on androgens for growth (6). However, prolonged use of androgen deprivation therapy (ADT) renders most hormone-sensitive prostate cancers (HSPCs) into lethal castration-resistant prostate cancer (CRPC). The defining characteristic of CRPC is the ability to grow in the androgen-poor environment created by ADT. A large subset of CRPC is characterized by restored AR signaling (7). Subsequent improved AR targeting with therapeutics such as abiraterone and enzalutamide has led to

life-extending advances for the treatment of CRPC (8, 9). Nevertheless, the disease remains uniformly fatal. Moreover, these potent inhibitors of AR and androgen metabolism have remodeled the phenotypic landscape of CRPC, resulting in a rise in lethal AR-deficient prostate cancers (10, 11).

In parallel studies, it has been shown that the process of translation initiation is a critical driver of prostate cancer pathogenesis. In particular, the cap-dependent translation initiation factor and oncogene eukaryotic initiation factor 4E (eIF4E) is necessary for the genesis and progression of prostate cancer mediated by loss of the tumor suppressor phosphatase and tensin homolog (PTEN) and may be a driver of drug resistance (12, 13). However, the fundamental question remains: How do AR and the translation initiation complex interplay? This is a critical issue because, to date, no inhibitors targeting translation regulators have shown broad efficacy in patients with prostate cancer (14–16).

We discovered a cell-autonomous mechanism by which AR inhibits translation initiation through the eIF4E-binding protein 1 (4EBP1), which limits eIF4F translation initiation complex formation and the proliferative capacity of cells *in vivo*. We also show that loss of AR increases eIF4F assembly to drive the translation of a network of pro-proliferation mRNAs that share a conserved and functional guanine-rich motif. This network is required for enhanced tumor growth in the setting of low AR. Moreover, we demonstrate that in comparison to AR-intact prostate cancer, AR-low prostate cancer has a greater physiologic dependence on eIF4F hyperactivity, which represents a druggable vulnerability. Pharmacologic and genetic disruption of the eIF4F complex decreases tumor growth and improves survival *in vivo*. As such, we have identified a link between mRNA transcription and translation that defines a specific treatment-resistant form of prostate cancer and is particularly vulnerable to translation inhibition.

¹Divisions of Human Biology and Clinical Research, Fred Hutchinson Cancer Research Center, Seattle, WA 98109, USA. ²Department of Medicine, Division of Gerontology and Geriatric Medicine, University of Washington, Seattle, WA 98104, USA. ³Comparative Medicine, Fred Hutchinson Cancer Research Center, Seattle, WA 98109, USA. ⁴Department of Urology, University of Washington, Seattle, WA 98115, USA. ⁵Human Oncology & Pathogenesis Program, Memorial Sloan Kettering Cancer Center, New York, NY 10065, USA. ⁶Department of Urology, Memorial Sloan Kettering Cancer Center, New York, NY 10065, USA. ⁷Departments of Medicine and Genome Sciences, University of Washington, Seattle, WA 98195, USA.

*These authors contributed equally to this work.

†Corresponding author. Email: ahsieh@fredhutch.org

RESULTS**AR regulates protein synthesis through 4EBP1**

To determine the impact of AR on protein synthesis, we used the *Probasin-cre;Pten^{LoxP/LoxP}* prostate cancer mouse model (herein referred to as *Pten^{L/L}*), where tissue-specific loss of *Pten* causes phosphatidylinositol 3-kinase (PI3K) pathway hyperactivation and prostate cancer formation (17). To modulate AR protein abundance, we castrated the mice, which led to a marked decrease in AR protein in each of the four lobes of the murine prostate (fig. S1, A to C). Moreover, we confirmed the functional impact of castration on AR activity by RNA sequencing (RNA-seq) (fig. S1D and table S1). Using a puromycin incorporation assay, we measured de novo protein synthesis in intact (noncastrate) and castrate *Pten^{L/L}* mice. We observed that castrate *Pten^{L/L}* mice exhibit a 30% increase in de novo protein synthesis on a per cell basis compared to intact *Pten^{L/L}* tumors (Fig. 1A). These findings indicate that AR negatively regulates protein synthesis, which is derepressed in the context of low AR protein abundance.

Next, we sought to determine how AR controls protein synthesis dynamics. Translation initiation mediated by the eIF4F complex is a critical driver of protein synthesis and cell proliferation (18, 19). This complex is composed of the oncogene eIF4E, which binds to the 5' cap of mRNA, the scaffolding molecule eIF4G, and the RNA helicase eIF4A (20–22). In addition, 4EBP1 is an antagonist of translation initiation and prevents eIF4F complex formation by binding to the dorsal and lateral surfaces of eIF4E (Fig. 1B) (23). 4EBP1 is phosphorylated and inhibited by the mechanistic target of rapamycin (mTOR) kinase (24). Translation initiation dynamics are strongly influenced by the stoichiometry of the translation initiation components eIF4E, eIF4G, eIF4A, and 4EBP1 (25). To determine the relationship between AR-low prostate cancer and eIF4F-mediated translation, we conducted quantitative immunofluorescence and Western blot analysis of these key translation initiation components in intact and castrate *Pten^{L/L}* mice. We observed no increase in eIF4E, eIF4G, or eIF4A protein abundance (Fig. 1C and fig. S1, E and F). However, 4EBP1 protein decreased in castrate mice relative to intact mice (Fig. 1C and fig. S1, C and E). Therefore, castration-induced low AR abundance results in a decrease in the translation inhibitor 4EBP1.

To determine whether the relationship between AR and 4EBP1 is particular to the *Pten^{L/L}* mouse model or a more general principle of prostate cancer, we used human LNCaP prostate cancer cells in which AR has been stably knocked down by short hairpin RNA and counterselected for using an AR-regulated suicide gene [herein referred to as APIPC (AR program-independent prostate cancer) cells] (11). Comparing APIPC cells to their isogenic parental AR-positive cells, we found that 4EBP1 protein expression substantially decreased in the absence of AR (Fig. 1D). Next, we asked whether AR protein expression also correlates with 4EBP1 protein expression in human prostate cancer. We evaluated 29 CRPC LuCaP patient-derived xenograft (PDX) models for AR and 4EBP1 protein abundance. We found a positive correlation ($R = 0.376$, $P = 0.02$) between AR and total 4EBP1 protein expression in these specimens, which was independent of genomic *PTEN* status (Fig. 1E and fig. S1, G and H). Together, these findings demonstrate that AR strongly correlates with 4EBP1 in both mice and humans.

AR directs *4ebp1* transcription through an ARE encoded in intron 1

The finding that 4EBP1 protein expression consistently correlates with AR protein in three models of advanced prostate cancer

(Fig. 1, C to E) drove us to question how AR regulates 4EBP1 abundance. Because AR is a transcription factor, we asked whether it regulates 4EBP1 directly through DNA-based mechanisms or indirectly through translation or protein decay (turnover). To determine whether AR affects 4EBP1 protein synthesis rates, we measured the amount of ribosome-protected *4ebp1* mRNA compared to total *4ebp1* mRNA through in vivo ribosome profiling (fig. S2, A and B) (26, 27). We observed no difference in *4ebp1* mRNA translation efficiency between intact and castrate *Pten^{L/L}* mice (fig. S2C). To investigate whether 4EBP1 protein turnover is sensitive to AR protein expression, we examined the phosphorylation status of 4EBP1 at T37/46, which is associated with its degradation (28). Western blot analysis revealed no increase in phosphorylation at those sites (fig. S1E). In addition, we also measured 4EBP1 degradation rates using cycloheximide in *Pten^{L/L}* primary prostate cancer cells grown with or without dihydrotestosterone (DHT). We observed no difference in 4EBP1 turnover rates between intact and castrate *Pten^{L/L}* cells (fig. S2D).

Next, we considered a transcription-based mechanism. We found that in all three model systems (*Pten^{L/L}* mouse model, APIPC human cell line, and LuCaP PDX models), *4ebp1* decreases at the mRNA level in the setting of low AR (Fig. 1F and fig. S2, E and F), which was not further affected by maximal AR blockade (fig. S2G). Moreover, we observed the same phenomenon in four different human prostate cancer cell lines (fig. S3, A and B). As such, we suspected that *4ebp1* is an AR-responsive gene. To determine whether AR regulates *4ebp1* mRNA expression, we reintroduced androgens to *Pten^{L/L}* primary cells derived from castrate mice to restore AR protein expression and activity. This resulted in a complete rescue of *4ebp1* mRNA back to AR-intact levels and a decrease in de novo protein synthesis (Fig. 1G and fig. S3, C and D). These findings suggested that AR may directly control the transcription of *4ebp1*. To determine whether AR binds the *4ebp1* genomic locus in vivo, we analyzed AR chromatin immunoprecipitation sequencing (ChIP-seq) from *Pten^{L/L}* mice (29). We found that AR binds to the first intron of *4ebp1*, which encodes a putative ARE (fig. S4A). This was also observed in wild-type murine prostate, where knockout of AR also decreased *4ebp1* mRNA, and in the LNCaP human prostate cancer cell line (fig. S4, B to D).

To determine the functionality of this element, we cloned the 347 bases encompassing the ChIP-seq peak including the putative ARE into a luciferase reporter construct and found that it was markedly responsive to androgen stimulation in LNCaP prostate cancer cells (Fig. 1H). Next, we deleted the 15–base pair ARE and found that this blunted the response to androgen stimulation (Fig. 1H and fig. S4E). We also cloned a homologous region of the human *4EBP1* locus into the luciferase reporter construct and found that it too increased luciferase activity in response to androgens (fig. S4F). Together, these findings reveal that *4ebp1* is controlled by AR via an ARE encoded within the first intron in both mice and humans.

4EBP1 protein abundance dictates eIF4E-eIF4G interaction dynamics and proliferation in a cell-autonomous manner in AR-low prostate cancer

Our observations suggest that AR may control translation initiation complex formation in vivo. To test this hypothesis, we optimized proximity ligation assays for eIF4E-eIF4G interactions and eIF4E-4EBP1 interactions (Fig. 2A) (30). In tumors from castrate *Pten^{L/L}* mice, we found that eIF4E-eIF4G interactions increase, whereas eIF4E-4EBP1 interactions decrease compared to those from intact mice (Fig. 2B). This was also confirmed by the cap-binding assay (fig. S5A).

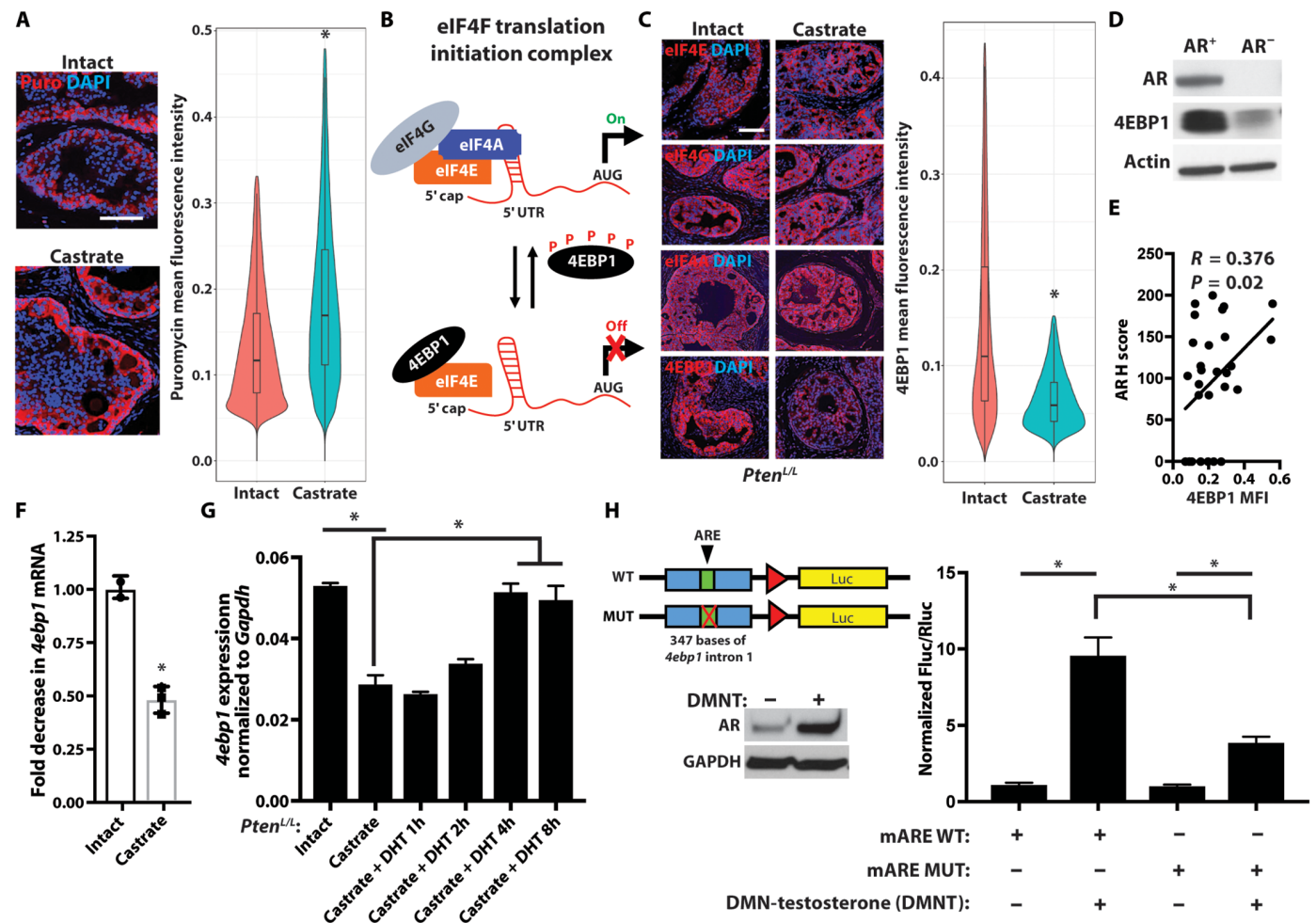


Fig. 1. AR controls translation initiation via a cis-element encoded within the *4ebp1* locus. (A) Representative puromycin immunofluorescence for de novo protein synthesis in vivo in intact and 8-week castrate *Pten^{L/L}* ventral prostates (left). Violin plot of per cell quantitation of puromycin mean fluorescence intensity. The height of the plot represents the range of new protein synthesis observed, and the width represents the number of cells at each fluorescence intensity [right; intact, $n = 3$ (46,711 cells quantified); castrate, $n = 4$ (73,237 cells quantified); $*P < 2.2 \times 10^{-16}$, t test]. DAPI, 4',6'-diamidino-2-phenylindole. (B) Simplified schematic of the eIF4F translation initiation complex composed of eIF4E, eIF4G, and eIF4A with the inhibitor of the complex, 4EBP1 (P, phosphorylation; AUG, start codon). (C) Representative immunofluorescence for eIF4E, eIF4G, eIF4A, and 4EBP1 in intact and 8-week castrate *Pten^{L/L}* ventral prostates (left). Violin plot of per cell quantitation of 4EBP1 mean fluorescence intensity [right; intact, $n = 6$ (148,974 cells quantified); castrate, $n = 5$ (111,046 cells quantified); $*P < 2.2 \times 10^{-16}$, t test]. (D) Representative Western blot for AR, 4EBP1, and actin in human AR⁺ parental and AR⁻ APIC (AR program-independent prostate cancer) cells. (E) Correlation plot of 29 human nonneuroendocrine CRPC LuCaP prostate cancer PDX models comparing AR protein content (y axis, AR H score) and 4EBP1 protein expression [x axis, 4EBP1 mean fluorescence intensity (MFI)] ($R = 0.376$, $P = 0.02$, Spearman's correlation). (F) *4ebp1* mRNA expression by RNA-seq in intact and 8-week castrate *Pten^{L/L}* ventral prostates (intact, $n = 2$; castrate, $n = 3$; $*P = 0.002$, t test). (G) *4ebp1* mRNA expression by qPCR in primary intact (DHT⁺) and castrate (DHT⁻) *Pten^{L/L}* prostate cancer cells. DHT (1 nM) was added back to castrate cells over the indicated time points (three biological replicates; $*P < 0.05$, t test). (H) Schematic of the wild-type (WT) and mutant (MUT) mouse *4ebp1* intron reporter constructs cloned into the pGL4.28 vector (red triangle, minimal promoter region; Luc, firefly luciferase). Representative Western blot of AR upon addition of testosterone analog dimethylnortestosterone (DMNT) in LNCaP cells (left). Luciferase assay of the putative wild-type and mutated (MUT) mouse *4ebp1* androgen response element (mARE) [right; six biological replicates; $*P < 0.0001$, analysis of variance (ANOVA)]. Scale bars, 100 μ m. Data are presented as means \pm SEM.

Thus, low AR alters the balance between eIF4E-4EBP1 inhibitory complexes and eIF4E-eIF4G initiation complexes, resulting in a net increase in eIF4F translation initiation complex formation and an increase in protein synthesis (Figs. 1A and 2B).

Next, we sought to determine the physiologic consequences of decreasing AR-4EBP1 while increasing eIF4F translation initiation complex formation in *Pten^{L/L}* mice. We observed that long-term castrated *Pten^{L/L}* mice exhibit increased tumor growth and cell proliferation and more aggressive disease (Fig. 2, C and D, and fig. S5B). This was independent of phenotypic changes such as neuroendocrine

differentiation (fig. S5, C and D) or reengagement of the AKT or mitogen-activated protein kinase (MAPK)-interacting serine/threonine-protein kinase 1 and 2 (MNK1/2) signaling pathways (as measured by AKT or eIF4E phosphorylation, respectively) that can increase translation initiation (fig. S5, E to G) (31, 32). We next determined whether the relationship between AR and 4EBP1 is intrinsic or extrinsic to prostate cancer epithelial cells. Using low-passage primary intact (DHT⁺) and castrate (DHT⁻) *Pten^{L/L}* cells, we found that, similar to our key in vivo findings, primary intact *Pten^{L/L}* cells do not express PTEN or neuroendocrine markers (Fig. 2E and fig. S5H). Moreover,

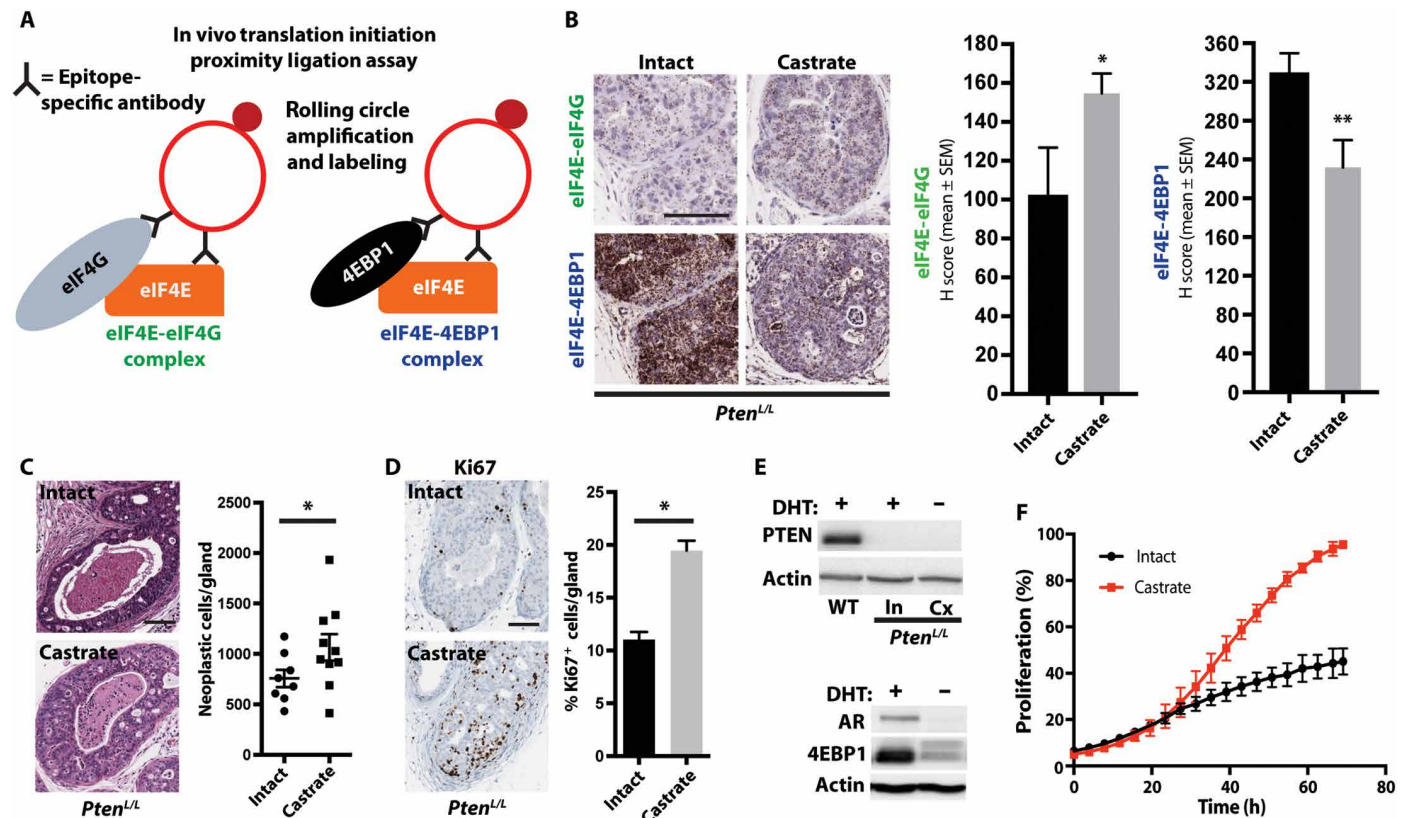


Fig. 2. 4EBP1 expression controls eIF4E-eIF4G interaction dynamics and proliferation in a cell-autonomous manner. (A) Schematic of the eIF4E-eIF4G and eIF4E-4EBP1 proximity ligation assays, which allow for the quantification of eIF4F translation initiation complexes and 4EBP1 inhibitory complexes in vivo. (B) Representative images of the eIF4E-eIF4G and eIF4E-4EBP1 proximity ligation assays in intact and 8-week castrate *Pten^{L/L}* ventral prostates (left). Quantification of the proximity ligation assay (right; intact, $n=6$; castrate, $n=7$; $*P=0.03$ and $**P=0.009$, t test). (C) Representative hematoxylin and eosin staining of intact and 8-week castrate *Pten^{L/L}* ventral prostates (left) with quantification (right; intact, $n=8$; castrate, $n=10$; $*P=0.04$, t test). (D) Representative Ki67 staining of intact and 8-week castrate *Pten^{L/L}* ventral prostates (left panel) with quantification [right panel: intact, $n=7$ (151 glands quantified); castrate, $n=9$ (206 glands quantified); $*P < 0.0001$, t test]. (E) Representative Western blot for PTEN and actin in wild-type, intact *Pten^{L/L}*, and 8-week castrate *Pten^{L/L}* primary organoids (top). Representative Western blot for AR, 4EBP1, and actin in intact *Pten^{L/L}* and 8-week castrate *Pten^{L/L}* primary organoids (bottom panel). (F) Growth curves of intact and castrate *Pten^{L/L}* primary cells (three biological replicates; $P=0.03$, t test). Scale bars, 100 μ m. Data are presented as means \pm SEM.

castrate cells expressed very low amounts of AR and 4EBP1 protein and proliferated faster than intact cells (Fig. 2, E and F). These findings demonstrate that a decrease in AR protein can diminish 4EBP1 abundance and increase cell proliferation in a cell-autonomous manner. Together, these findings mimic, in part, an emerging subset of CRPC patients with low AR protein expression and resistance to second-generation therapeutics such as enzalutamide (11).

AR and eIF4F-mediated mRNA-specific translation controls a regulon of functional cell proliferation regulators

Given that AR-low prostate cancer increases eIF4F complex formation and de novo protein synthesis (Figs. 1A and 2B), we next asked whether this affects the translation of all mRNAs or a subset of mRNAs. To do so, we conducted ribosome profiling of tumors from both intact and castrate *Pten^{L/L}* mice to identify differentially translated mRNAs (fig. S2A). Castration and increased eIF4F complex formation were associated with an increase in the translation efficiency of a subset of 697 mRNAs as opposed to all mRNA species (\log_2 fold change, ≥ 0.75 ; P value $< 2.2 \times 10^{-16}$) (Fig. 3A). This finding raised the important question of what makes these specific mRNAs particularly sensitive to increases in eIF4F activity.

A major determinant of translation initiation rates is the composition of the 5' untranslated region (5'UTR) of an mRNA (33). We observed that the translationally up-regulated mRNAs have a higher guanine-cytosine (GC) content and are more thermodynamically stable compared to 19,009 control 5'UTRs (Fig. 3B). There was no substantial difference in 5'UTR length (fig. S6A). Together, these findings suggest that eIF4F-sensitive mRNAs may have a cis-regulatory element encoded within the 5'UTR. We conducted a motif analysis and discovered a guanine-enriched sequence that we named the guanine-rich translational element (GRTE) (Fig. 3C and table S2). The GRTE was present in 66.8% of up-regulated mRNAs and 39.6% of genomic 5'UTR sequences ($P = 6.32 \times 10^{-14}$) and was distinct from the previously described mTOR-sensitive pyrimidine-rich translational element (PRTE) cis-regulatory element (fig. S6, B and C) (27). To determine whether GRTE-containing 5'UTRs were responsive to fluctuations in eIF4F activity, we cloned the 5'UTRs of *Klf5* and *Denr*, which have this element, into luciferase reporter constructs and also generated GRTE deletion mutants (fig. S6D). This was subsequently transduced into PC3-4EBP1^M prostate cancer cells in which doxycycline can induce the expression of a nonphosphorylatable form of 4EBP1 to inhibit eIF4F complex formation (fig. S6E) (27).

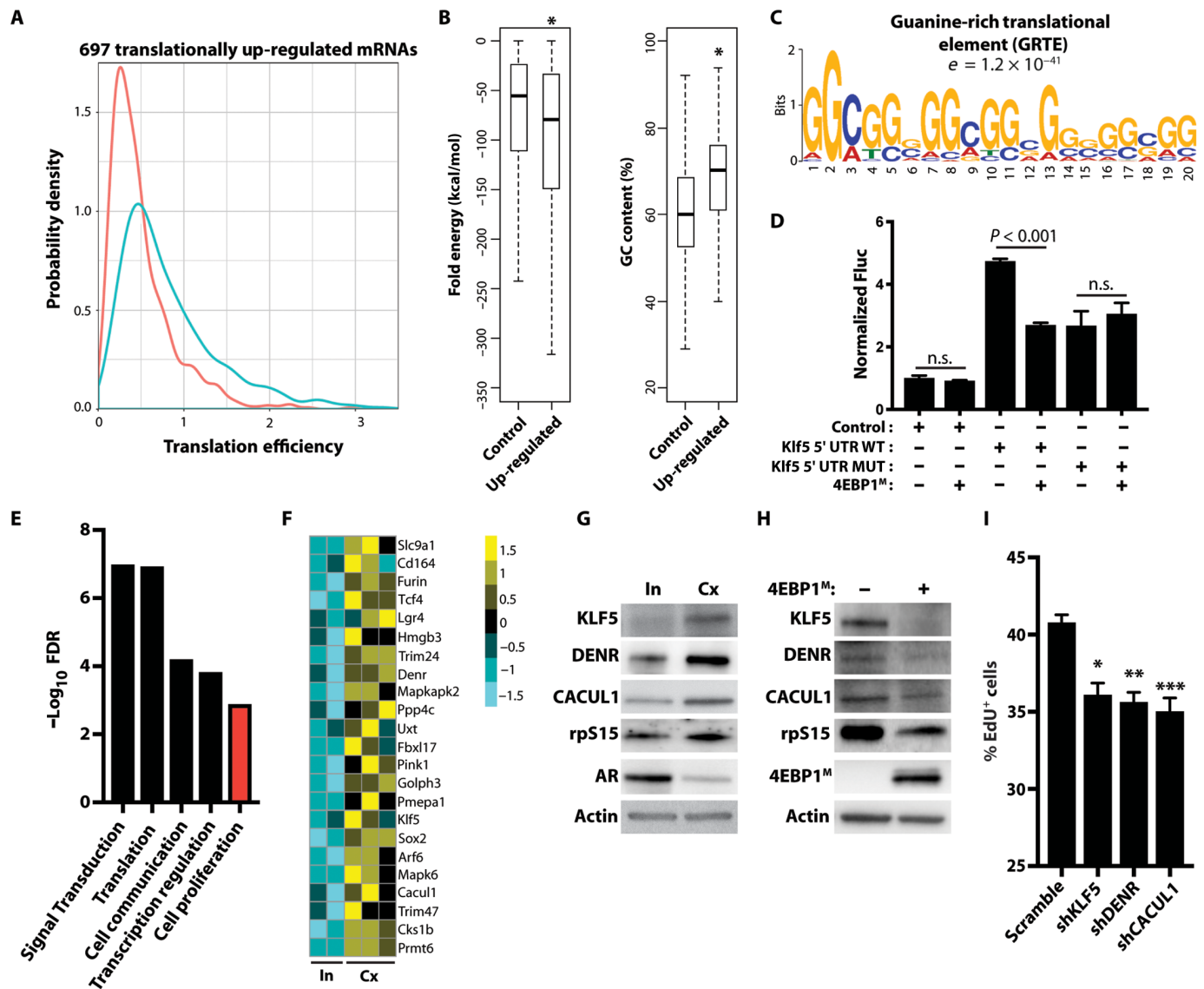


Fig. 3. AR and eIF4F-mediated mRNA-specific translation controls a regulon of functional cell proliferation regulators. (A) Probability density graph of 697 translationally up-regulated mRNAs between intact ($n = 2$) and castrate ($n = 3$) *Pten*^{L/L} ventral prostates. Translation efficiency, ribosome-bound mRNA/total mRNA ($P < 2.2 \times 10^{-16}$, Kolmogorov-Smirnov test). (B) Folding energy ($*P = 0.004339$) and %GC content ($*P < 2.2 \times 10^{-16}$) between 5'UTRs of control mRNA ($n = 19,009$) and up-regulated mRNA ($n = 187$, t test). Whiskers represent 1.5 times the interquartile range. (C) The GRTE consensus sequence ($e = 1.2 \times 10^{-41}$). (D) Luciferase assay of the control vector, wild-type *Klf5* 5'UTR luciferase construct, and its GRTE deletion mutant with or without 4EBP1^M induction. Luciferase assay was normalized to *luc* and *RPS19* mRNA (n.s., not statistically significant; $n > 3$ biological replicates per condition, t test). (E) Gene set enrichment analysis of the translationally up-regulated mRNA (\log_2 fold change, ≥ 0.75 ; FDR < 0.1) in castrate *Pten*^{L/L} mice. (F) Heatmap of translationally up-regulated proliferation regulators in AR-low prostate cancer (\log_2 fold change, ≥ 0.75 ; FDR < 0.1). (G) Representative Western blot analysis of KLF5, DENR, CACUL1, rpS15, AR, and actin in primary intact (In; DHT⁺) and castrate (Cx; DHT⁻) *Pten*^{L/L} organoids. (H) Representative Western blot analysis of KLF5, DENR, CACUL1, rpS15, AR, and actin in primary *Pten*^{L/L}; *4ebp1*^M organoids with or without 4EBP1^M induction. (I) Cell proliferation EdU incorporation assay in scramble, shKLF5, shDENR, or shCACUL1 castrate (DHT⁻) *Pten*^{L/L} primary cells (replicate of four to six per condition; $*P = 0.02$, $**P < 0.0001$, and $***P = 0.0003$, t test). Data are presented as means \pm SEM.

We observed that wild-type *Klf5* and *Denr* 5'UTRs displayed a decrease in luciferase activity upon induction of the 4EBP1^M. However, the non-insert control vector and the GRTE deletion *Klf5* and *Denr* 5'UTRs were both insensitive to eIF4F complex disruption (Fig. 3D and fig. S6F). Next, we sought to determine the specificity of the GRTE by generating wild-type and mutant luciferase reporters with the *Tcea1* 5'UTR, which has a guanine-enriched sequence but was not found to be translationally up-regulated by ribosome profiling (data file S1).

In this context, mutating the element had no impact on translation (fig. S6G). Together, these findings indicate that the GRTE is a specific 5'UTR cis-regulatory element that in part enables the enhanced translation of distinct mRNAs in the context of eIF4F hyperactivity.

We next asked whether the translationally up-regulated mRNAs identified by ribosome profiling organize into networks that may be responsible for specific phenotypes important for AR independence. Through gene set enrichment analysis, we found that these translationally

regulated mRNAs cluster into distinct biological processes including signal transduction, translation, cell communication, transcription regulation, and cell proliferation (Fig. 3E). This was corroborated at a gene-specific level. For example, a number of shared mTOR inhibitor-sensitive target genes were up-regulated in the AR-low setting, including *Pabpc1*, *Rps13*, *Rps15*, *Rpl7a*, and *Rpl14* (fig. S6, B and H) (27, 34). Furthermore, we also identified 23 putative regulators of cell proliferation that increased at the level of translation in castrate *Pten^{L/L}* mice (Fig. 3F). Together, these findings demonstrate that low AR and increased eIF4F complex formation may promote cancer progression through the translation of distinct networks of mRNAs.

To confirm that the putative proliferation regulators identified by ribosome profiling are controlled at the posttranscriptional level, we conducted Western blot and quantitative polymerase chain reaction (qPCR) analysis on a subset of targets including KLF5, a transcription factor critical for maintaining the proliferative capacity of cells; CACUL1, a cullin domain-containing protein that activates CDK2; and DENR, a translation reinitiation factor important for high-density cell proliferation (35–37). All three genes have at least one GRTE. As a positive control, we also analyzed the small ribosomal subunit protein rpS15. We found that castrate primary *Pten^{L/L}* organoids exhibited increases in the abundance of KLF5, DENR, CACUL1, and rpS15 proteins (Fig. 3G and fig. S7A). However, at the mRNA level, no increase was observed (fig. S7B). Together, these findings indicate that KLF5, DENR, and CACUL1 are regulated at the posttranscriptional level. To determine whether these genes are regulated by the eIF4F complex, we conducted a reciprocal experiment using organoids derived from castrate *Pten^{L/L}* mice, which also have a doxycycline-inducible 4EBP1^M. In this system, castration and prostate-specific loss of PTEN cause nonneuroendocrine AR-low prostate cancer, and doxycycline drives the prostate-specific expression of an inducible nonphosphorylatable *4ebp1* mutant transgene (herein referred to as *Pten^{L/L};4ebp1^M*; fig. S7C). Upon induction of the 4EBP1^M, which diminishes eIF4F complex assembly, we observed a marked decrease in the amounts of KLF5, DENR, CACUL1, and rpS15 proteins (Fig. 3H and fig. S7D). This did not result from a decrease in mRNA (fig. S7E). Thus, AR coordinates the translation of a distinct subset of mRNAs including a network of pro-proliferation regulators through aberrant eIF4F complex formation. To determine whether KLF5, DENR, and CACUL1 are necessary to drive the enhanced growth of AR-low CRPC, we used RNA interference to knock down each gene in castrate *Pten^{L/L}* primary prostate cancer cells (fig. S7F). Gene silencing of *Klf5*, *Denr*, and *Cacul1* resulted in a sustained decrease in EdU incorporation compared to a scramble control (Fig. 3I). Together, these findings demonstrate that AR-low prostate cancer exhibits an increase in protein synthesis through the translation of specific subsets of GRTE-containing mRNAs, including an eIF4F-sensitive pro-proliferation regulon, which drives the enhanced growth of AR-low prostate cancer.

Increased eIF4F complex formation is necessary for AR-low prostate cancer initiation and progression

Our findings raised the question of whether the increase in eIF4F complex formation is necessary for AR-low prostate cancer pathogenesis. To test this, we used the *Pten^{L/L};4ebp1^M* mouse model (fig. S7C). Using the eIF4E-eIF4G proximity ligation assay, we found that the 4EBP1^M decreases eIF4F complex formation by about 50% in vivo (fig. S8A). We castrated a cohort of *Pten^{L/L};4ebp1^M* mice and immediately initiated doxycycline treatment to induce the 4EBP1^M (Fig. 4A).

Eight weeks after induction, we observed a decrease in tumor volumes and cell proliferation in *Pten^{L/L};4ebp1^M* mice on doxycycline (Fig. 4, B and C). As such, increased eIF4F complex formation drives AR-low prostate cancer initiation and enhanced cell proliferation in vivo.

Next, we asked whether increased eIF4E-eIF4G interactions are necessary for AR-low prostate cancer progression. We first castrated *Pten^{L/L};4ebp1^M* mice and allowed AR-low tumors to grow over 12 weeks. Then, we randomized half of the cohort onto doxycycline for 12 weeks (Fig. 4D). In this experiment, we observed a 50% decrease in tumor weight, a decrease in cell proliferation, and a decrease in the formation of carcinoma in the doxycycline-treated group (Fig. 4, E to G, and fig. S8, B and C). Therefore, increased eIF4F complex formation also maintains the proliferative potential of established AR-low prostate cancer.

Therapeutic disruption of the eIF4E-eIF4G interaction in AR-low prostate cancer inhibits tumor growth and extends survival

A question that arises from our findings is whether AR-low prostate cancer is more addicted to alterations of the eIF4F complex compared to AR-normal or AR-intact prostate cancer. This has potential clinical implications because no targeted therapies against translation regulators have been broadly efficacious in patients with prostate cancer (14–16). To address this question, we used *Pten^{L/L};4ebp1^M* primary cells grown with or without DHT. Cells were treated with doxycycline to induce 4EBP1^M to near equivalent expression between the intact and castrate settings (fig. S9A). We found that AR-low prostate cancer cell proliferation was more decreased by inhibition of eIF4F compared to AR-intact cells (Fig. 5A). This increased sensitivity was also observed in vivo (fig. S9B). As such, AR-low prostate cancer may represent an emerging subtype of treatment-resistant prostate cancer with a heightened addiction to increased eIF4E-eIF4G interactions.

These findings raise the possibility that the eIF4F complex is a therapeutic target in CRPC that is more functionally relevant in the context of low AR. This is further supported by the finding that patients with end-stage CRPC and human CRPC PDX models exhibit lower 4EBP1 protein abundance when AR expression is low (Figs. 1E and 5B). In contrast, the positive correlation between AR and 4EBP1 protein expression was not observed in patients with treatment-naïve HSPC (fig. S9C). To delineate the dependence on eIF4F in AR-low prostate cancer, we used 4E1RCat, 4E2RCat, and 4EGI-1, three small molecules that can disrupt the formation of the eIF4E-eIF4G complex (Fig. 5C) (38–40). We found that drug concentrations with negligible effects on cell proliferation in primary intact (DHT⁺) *Pten^{L/L}* cells induced profound changes in primary castrate (DHT⁻) *Pten^{L/L}* cells (Fig. 5, D and E, and fig. S10A). Next, we asked whether human prostate cancer cells exhibit a similar therapeutic profile. We treated parental (AR⁺) or APIPC (AR⁻) cells with 4E2RCat or 4EGI-1. Similar to our findings in the murine models, AR-null APIPC cells were more sensitive to eIF4E-eIF4G disruption (Fig. 5, F and G, and fig. S10B).

Given these promising in vitro findings, we next tested this hypothesis using in vivo models of advanced AR-low prostate cancer. Specifically, we conducted preclinical trials using 4E1RCat, an eIF4E-eIF4G disruptor with in vivo efficacy (Fig. 6A) (38), on the APIPC xenograft model and the AR-null nonneuroendocrine LuCaP 173.2 PDX model. In both studies, we observed a marked decrease in tumor growth and improvement in survival without overt toxicity

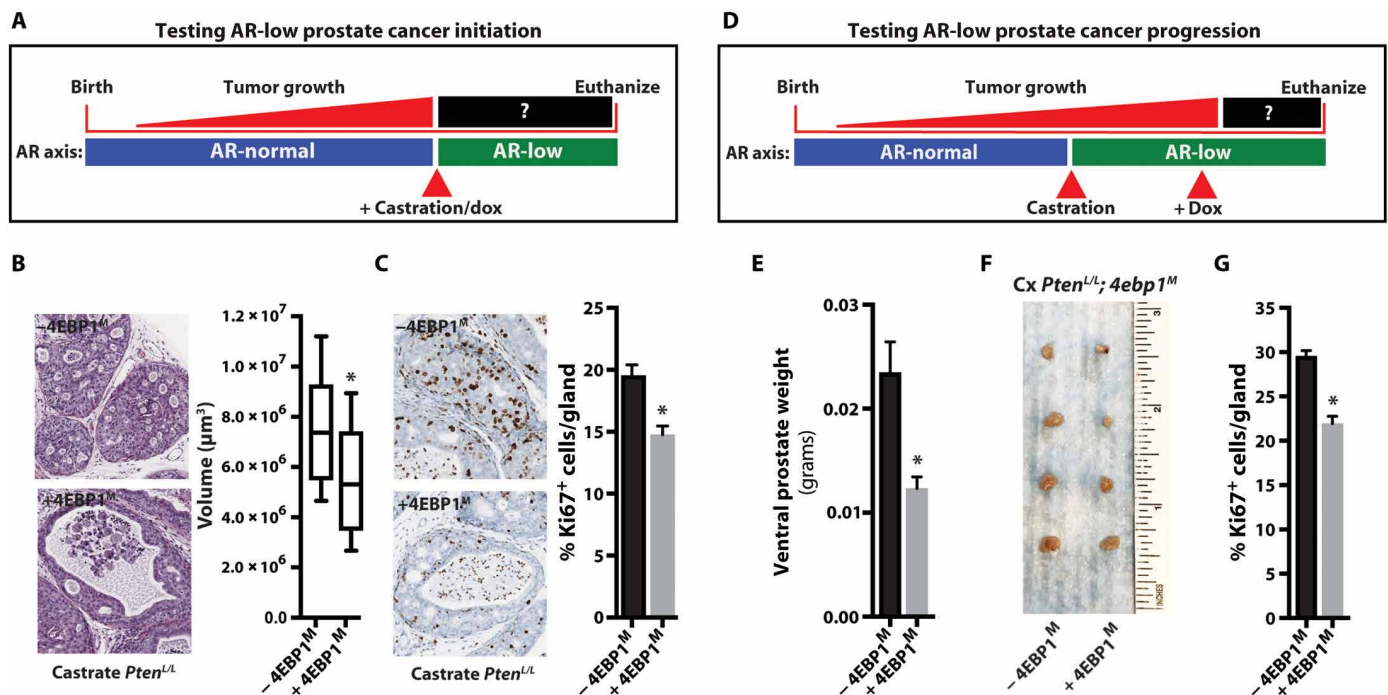


Fig. 4. Increased eIF4F complex formation is necessary for AR-low prostate cancer initiation and progression. (A) Schematic diagram of testing the impact of inhibiting eIF4F complex formation on AR-low prostate cancer initiation. *Pten^{L/L};4ebp1^M* mice were castrated and immediately put on vehicle or doxycycline (dox) for 8 weeks. (B) Representative hematoxylin and eosin staining of vehicle-treated (-4EBP1^M) and doxycycline-treated (+4EBP1^M) *Pten^{L/L};4ebp1^M* ventral prostates (left). Quantification of tumor volumes after 8 weeks of inhibition of eIF4F complex formation started immediately after castration (right; vehicle, $n = 9$; doxycycline, $n = 9$; $*P = 0.04$). (C) Representative Ki67 staining of vehicle-treated (-4EBP1^M) and doxycycline-treated (+4EBP1^M) *Pten^{L/L};4ebp1^M* ventral prostates (left). Ki67 quantification after 8-week castration and concurrent vehicle or doxycycline treatment [right; vehicle, $n = 9$ (205 glands quantified); doxycycline, $n = 8$ (169 glands quantified); $*P < 0.0001$, t test]. (D) Schematic diagram of testing the impact of inhibiting eIF4F assembly on AR-low prostate cancer progression. *Pten^{L/L};4ebp1^M* mice were castrated and allowed to form AR-low tumors for 12 weeks followed by an additional 12-week vehicle or doxycycline treatment. (E) *Pten^{L/L};4ebp1^M* ventral prostate weights after a 12-week castration followed by an additional 12-week vehicle or doxycycline treatment (vehicle, $n = 10$; doxycycline, $n = 9$; $*P = 0.0018$, t test). (F) Representative images of *Pten^{L/L};4ebp1^M* ventral prostates with or without *4ebp1^M* induction in the progression experiment. (G) *Pten^{L/L};4ebp1^M* ventral prostate Ki67 quantification after a 12-week castration followed by an additional 12-week vehicle or doxycycline treatment [vehicle, $n = 9$ (197 glands quantified); doxycycline, $n = 7$ (139 glands quantified); $*P < 0.0001$, t test]. Scale bars, 100 μm . Data are presented as means \pm SEM.

to mice (Fig. 6, B to E, and fig. S11, A and B). To determine whether the therapeutic impact was specific to tumors with lower AR protein expression, we also treated AR⁺ parental APIPC xenograft mice with 4E1RCat. This isogenic AR⁺ xenograft model was completely insensitive to the eIF4E-eIF4G disruptor (Fig. 6F and fig. S11C). Thus, patients with AR-deficient prostate cancer may benefit most from eIF4F complex disruption. Furthermore, eIF4F disruption may also improve the efficacy of maximal AR blockade therapies such as enzalutamide used in patients with new onset CRPC (fig. S11, D to F).

DISCUSSION

Here, we show through mouse genetics and molecular analyses that a relationship between AR signaling and translation initiation is instrumental in maintaining protein synthesis rates in prostate cancer. In particular, AR represses protein synthesis by controlling the abundance of the translation initiation inhibitor 4EBP1 and eIF4F complex formation (fig. S12). This conclusion is supported by our finding that AR binds to an ARE encoded within the first intron of *4ebp1* and promotes its transcription in both normal and cancerous prostates. Reduction or genetic ablation of AR impairs *4ebp1*

expression, leading to a substantial increase in the protranslation eIF4E-eIF4G complex resulting in greater translation initiation. Using the *Pten^{L/L};4ebp1^M* mouse model, we further demonstrated that eIF4F complex formation is essential to initiate and maintain the proliferative potential of AR-low prostate cancer. These findings are clinically relevant because the advent of potent inhibitors of AR or androgen biosynthesis over the past decade has resulted in a 2.5-fold increase of highly treatment-resistant prostate cancer characterized by AR deficiency (11). Our finding reveals that derepression of translation initiation represents a bypass tract by which prostate cancers deprived of androgen signaling can maintain their proliferative potential leading to AR independence.

An important concept arising from our work is that AR negatively regulates mRNA translation initiation. This raises the question of why this mechanism exists in the first place. One explanation is that AR promotes normal prostate epithelial cell differentiation and may use 4EBP1 to rapidly inhibit protein synthesis, cell growth, and proliferation to allow for tissue maintenance. This was partially demonstrated in prostate epithelial-specific AR knockout mice, which exhibit impaired differentiation and increased cell proliferation that can be rescued through the transgenic expression of a constitutively activated AR (41). It remains to be determined whether this phenotype

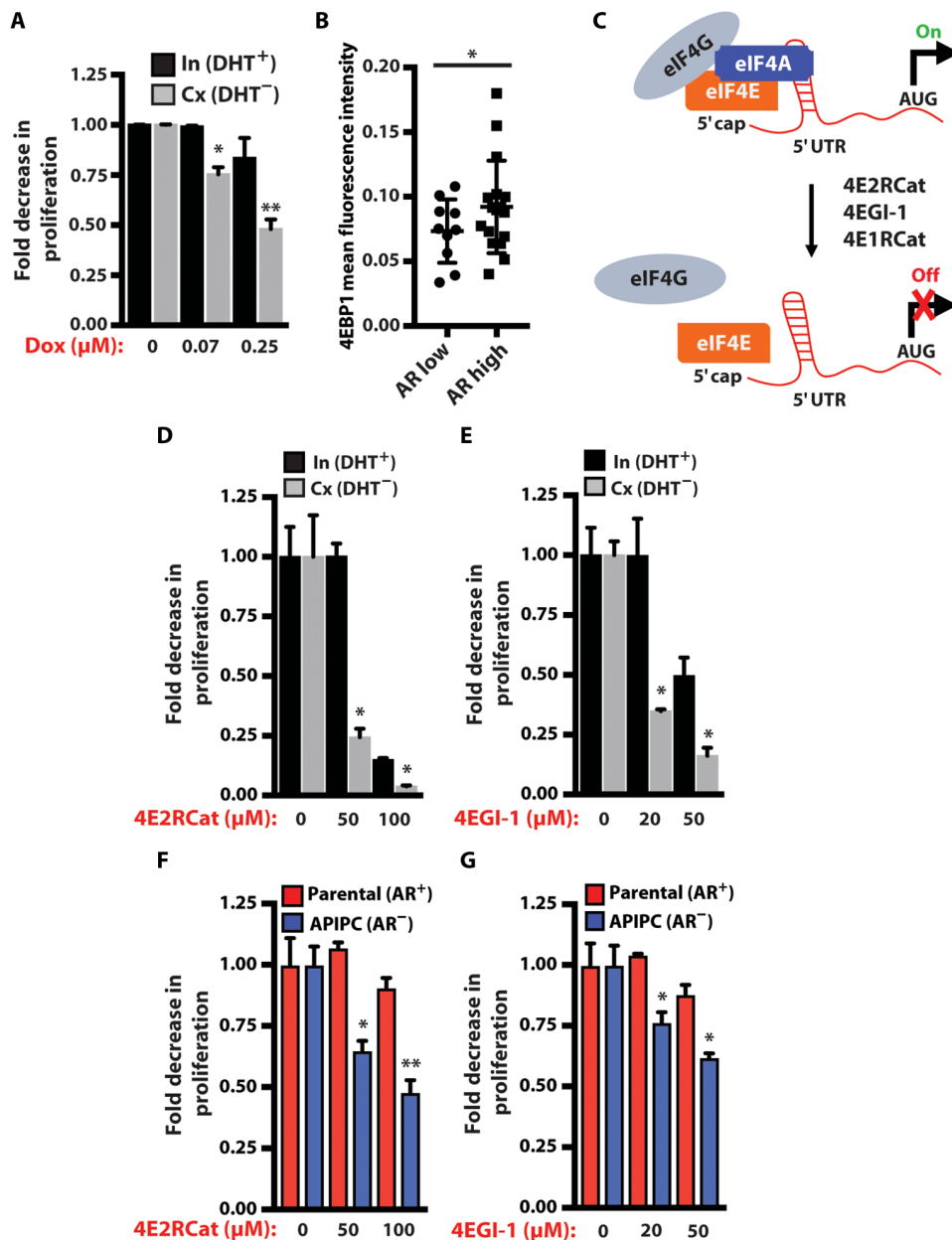


Fig. 5. AR-low prostate cancer is more sensitive to disruption of the eIF4E-eIF4G interaction than AR-intact prostate cancer. (A) Intact and castrate *Pten*^{L/L};*4ebp1*^M primary prostate cancer cells treated with doxycycline for 48 hours. Proliferation was measured using the IncuCyte platform (assay completed in triplicate; **P* = 0.0026 and ***P* = 0.03, *t* test). (B) 4EBP1 protein immunofluorescence quantification of a tissue microarray composed of end-stage metastatic CRPC patient specimens classified by AR protein expression (two to four tumors sampled per patient; AR low, *n* = 10; AR high, *n* = 17; **P* = 0.0089, *t* test). (C) Simplified schematic of the mechanism of action of 4E1RCat, 4E2RCat, and 4EGI-1, which disrupt the eIF4E-eIF4G interaction. (D) Intact and castrate *Pten*^{L/L} cells treated with 4E2RCat for 48 hours. Proliferation was measured using the IncuCyte platform (assay completed in triplicate; **P* < 0.0001, *t* test). (E) Intact and castrate *Pten*^{L/L} cells treated with 4EGI-1 for 48 hours. Proliferation was measured using the IncuCyte platform (assay completed in triplicate; **P* = 0.002, *t* test). (F) AR⁺ parental and AR⁻ APIPC prostate cancer cells treated with 4E2RCat for 48 hours. Proliferation was measured using the IncuCyte platform (assay completed in triplicate; **P* < 0.0001 and ***P* = 0.0003, *t* test). (G) AR⁺ parental and AR⁻ APIPC prostate cancer cells treated with 4EGI-1 for 48 hours. Proliferation was measured using the IncuCyte platform (assay completed in triplicate; **P* = 0.0003, *t* test). Data are presented as means ± SEM.

is mediated by 4EBP1. Another possibility is that AR regulates metabolic homeostasis through 4EBP1. Alterations in testosterone and AR affect insulin sensitivity and energy metabolism in response to

a high-fat diet (42). In a similar manner, *4ebp1* and *4ebp2* knockout mice phenocopy the metabolic defects seen in AR-null or AR-low mice, and overexpression of 4EBP1 is sufficient to rescue the high-fat diet-induced metabolic defects but only in male mice (43, 44). Our finding that AR directly coordinates *4ebp1* expression provides a potential mechanistic basis for how hormone signaling directs tissue growth and metabolism. However, in the context of advanced enzalutamide- or abiraterone-resistant prostate cancer, low AR unleashes the translation initiation apparatus to drive previously inhibited gene networks that can be hijacked to overcome AR dependencies.

To determine the identity of the translational networks affected by a decrease in AR and an increase in eIF4F complex formation, we conducted ribosome profiling in intact and castrate *Pten*^{L/L} mice. Despite the 30% increase in overall protein synthesis in vivo, only 697 mRNAs demonstrated an increase in translation efficiency. These findings highlight that increasing eIF4F assembly does not affect every mRNA equally and that specific mRNAs are more sensitive to changes in translation initiation dynamics. This is in part due to enrichment for the GRTE cis-regulatory element encoded within the 5'UTRs of most of these up-regulated genes. The *Klf5* and *Denr* 5'UTRs have the GRTE and are sensitive to decreases in eIF4F complex formation. However, not all guanine-rich sequences are responsive to changes in eIF4F activity. For example, we also show that the *Tcea1* 5'UTR, which also encodes a guanine-rich motif but was not translationally up-regulated upon castration, does not exhibit a decrease in translation when the sequence is mutated. Together, these data indicate that the surrounding sequence context of the GRTE may also play a role in eIF4F hypersensitivity. Future studies are required to substantiate this hypothesis.

In addition to this shared sequence motif, we also observed that these up-regulated genes, identified by ribosome profiling, bin into distinct functional classes. We found enrichment for a network of translationally regulated mRNAs involved in cell proliferation. The functional diversity of these genes reveals

that eIF4F controls distinct cellular processes such as proliferation through coordinated regulation of transcription (KLF5), CDK function (CACUL1), and translation (DENR). As such, eIF4F-mediated

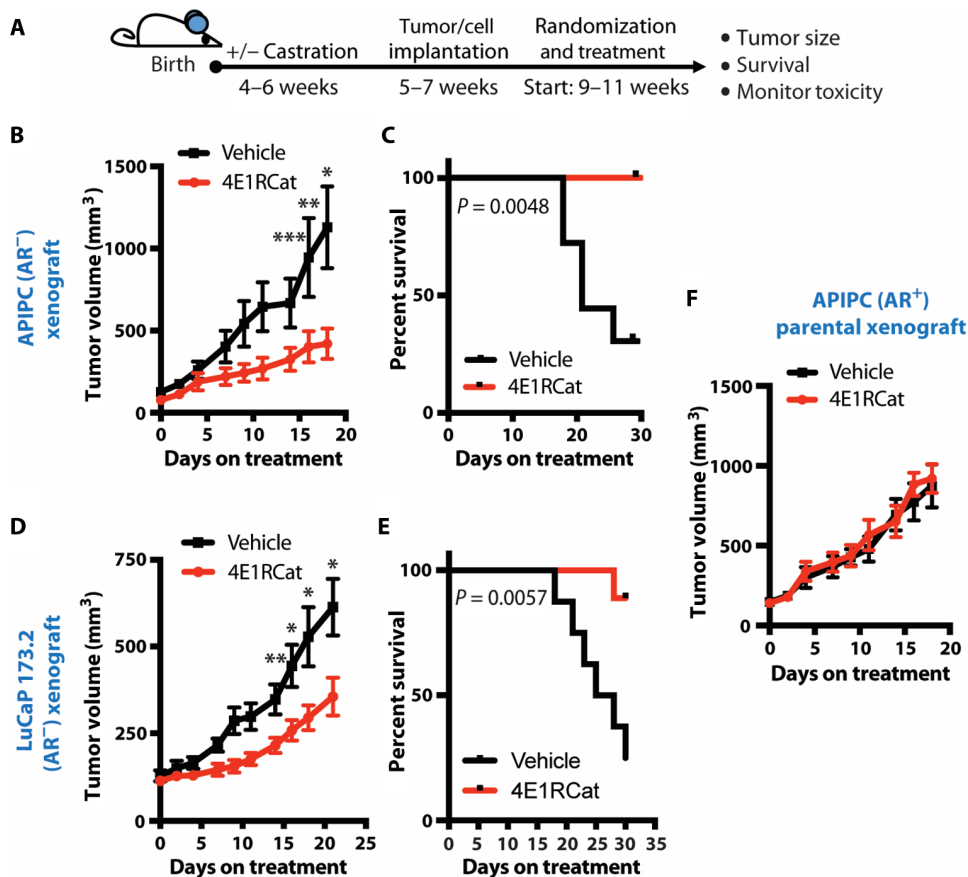


Fig. 6. Targeting the eIF4E-eIF4G interaction in AR-deficient prostate cancer decreases tumor growth and improves survival. (A) Schematic of the eIF4E-eIF4G interaction inhibitor preclinical trials. (B) AR⁻ APiPC xenograft preclinical trial testing the efficacy of 4E1RCat on AR-low prostate cancer tumor growth. Castrated mice were treated with 4E1RCat or vehicle (15 mg/kg; 4E1RCat-treated, $n=8$; vehicle-treated mice, $n=7$; * $P=0.0124$, ** $P=0.045$, and *** $P=0.05$, t test). (C) AR⁻ APiPC xenograft preclinical trial testing the impact of 4E1RCat on AR-low prostate cancer survival. Castrated mice were treated with 4E1RCat or vehicle (15 mg/kg; 4E1RCat-treated, $n=8$; vehicle-treated mice, $n=7$; $P=0.0048$, log-rank test). (D) LuCaP 173.2 PDX preclinical trial testing the efficacy of 4E1RCat on AR-low prostate tumor growth. Castrated mice were treated with 4E1RCat or vehicle (15 mg/kg; 4E1RCat-treated, $n=9$; vehicle-treated mice, $n=8$; * $P=0.02$ and ** $P=0.01$, t test). (E) LuCaP 173.2 PDX preclinical trial testing the impact of 4E1RCat in AR-low prostate cancer survival. Castrated mice were treated with 4E1RCat or vehicle (15 mg/kg; 4E1RCat-treated, $n=9$; vehicle-treated mice, $n=8$; $P=0.0057$, log-rank test). (F) AR⁺ parental APiPC xenograft preclinical trial testing the efficacy of 4E1RCat on AR⁺ prostate cancer tumor growth. Uncastrated mice were treated with 4E1RCat or vehicle (15 mg/kg; 4E1RCat-treated, $n=8$; vehicle-treated mice, $n=7$). Data are presented as means \pm SEM.

translation enables the networking of multiple molecular modules that converge on shared cellular processes that can be usurped in the context of AR-low prostate cancer. Our findings provide an example of how a DNA cis-element coordinates the function of a network of cis-regulatory element-containing mRNAs to drive a cellular process.

Last, we show that the eIF4E-eIF4G interaction represents a therapeutic vulnerability in AR-low prostate cancer (fig. S12). This has clinical implications because we observe that AR protein expression positively correlates with 4EBP1 abundance in patients with advanced-stage prostate cancer, and no therapeutics targeting translation regulators have demonstrated broad clinical efficacy to date (14–16). To demonstrate this dependence, we showed that AR-low prostate cancer is more sensitive to inhibition by the *4ebp1*^M transgene compared to AR-intact prostate cancer both in vitro and in vivo. Further-

more, using small-molecule disruptors of the eIF4F complex, we found that both human and murine models of AR-low prostate cancer depend on increased eIF4F complex formation to maintain their high proliferation rate more so than their AR-intact counterparts. Ultimately, targeting the eIF4F complex in human models of AR-low but not of AR-intact prostate cancer results in a decrease in tumor growth and an improvement in survival. Our study was limited to pre-clinical models given the paucity of translation initiation inhibitors currently in clinical trials for patients with prostate cancer with available clinical specimens. However, protein synthesis inhibitors are currently in development and are being tested in phase 1 and 2 clinical trials (NCT03616834 and NCT03690141). Together, this work provides a mechanistic rationale for patient stratification to emerging therapies that target the translation initiation machinery in prostate cancer. Our data suggest that prostate cancer patients with derepressed translation initiation, particularly in the AR-low setting, represent a growing patient population who should most benefit from emerging eIF4F-targeted therapeutics.

MATERIALS AND METHODS

Study design

The goals of this study were to delineate the functional relationship between AR signaling and the process of mRNA translation and to define the preclinical relevance of targeting protein synthesis based on AR status. This objective was accomplished by (i) mechanistically dissecting the functional relationship between AR and 4EBP1, (ii) using tissue-based ribosome profiling to identify and validate AR-controlled translationally regulated mRNAs, (iii) validating the relationship between AR and 4EBP1 in prostate cancer across multiple model systems, and (iv) conducting a series of in vitro and in vivo preclinical trials delineating the therapeutic efficacy of targeting eIF4E-eIF4G interactions in AR-low prostate cancer. For all experiments, our sample sizes were determined on the basis of experience and published literature, which historically showed that these in vivo models are highly penetrant and universally develop tumors. We used the maximum number of mice available for a given experiment based on the following criteria: the number of genetically engineered mouse models available for each age group and post-castration cohort and tumor availability after implantation of human tissue specimens and cell lines. For all studies, mice were randomly assigned to each treatment group. All pathology analyses were conducted by a blinded

veterinarian pathologist. The numbers of replicates are specified within each figure legend.

Mice

PB-cre mice were obtained from the Mouse Models of Human Cancer Consortium. *Pten^{L/L}* and *Rosa-LSL-rtTA* mice were obtained from the Jackson Laboratory. *TetO-4ebp1^M* mice were generated as previously described (12). All mice were maintained in the C57BL/6 background under specific pathogen-free conditions, and experiments conformed to the guidelines as approved by the Institutional Animal Care and Use Committee of Fred Hutchinson Cancer Research Center (FHCRC).

Surgical castration

Surgical castrations were performed with 4- to 6-month-old mice under isoflurane anesthesia. Postoperatively, mice were monitored daily for 5 days. To test CRPC initiation, doxycycline (Sigma-Aldrich) was administered in the drinking water at 2 g/liter immediately after castration, and euthanasia was performed 8 weeks after castration. To test CRPC progression, 12 weeks after castration, doxycycline was administered for 12 weeks, and euthanasia was performed 24 weeks after castration.

LuCaP, localized treatment-naïve HSPC, and metastatic CRPC tissue microarrays

The tissue microarrays were obtained from the University of Washington (UW) Genitourinary Cancer Research Laboratory. All patients consented, and samples were obtained under the UW Institutional Review Board–approved protocol 2341.

In vivo puromycinylation assay

Mice were injected intraperitoneally with 200 μ l of 2.5 mM puromycin (Thermo Fisher Scientific) and euthanized after 1 hour. Ventral prostates were formalin-fixed and paraffin-embedded. Conventional immunofluorescence against puromycin (Millipore) was performed as described in the Supplementary Materials with antigen retrieval at 95°C for 30 min and additional incubation with Mouse on Mouse Blocking Reagent (Vector Laboratories) for 1 hour at room temperature.

AR⁺ parental, AR⁻ AIPIC, and LuCaP 173.2 PDX 4E1RCat preclinical trials

AR⁺ parental and AR⁻ AIPIC cells (1×10^6) were resuspended in 1:1 Matrigel (Corning):RPMI 1640 (Gibco) and subcutaneously injected into the flanks of intact or castrate nonobese diabetic–severe combined immunodeficient IL2Ry^{null} mice, respectively. LuCaP 173.2 tumor chunks (1 mm \times 1 mm \times 1 mm) were implanted into the flank of castrate mice. Tumor volume was calculated using the formula $[L(W^2)]/2$, where L is the length of the tumor and W is the width. When tumors reached 100 mm³, animals were randomized to receive intraperitoneal injections of 4E1RCat (15 mg/kg per day; Selleckchem) or vehicle (5.2% polyethylene glycol, molecular weight 400 and 5.2% Tween 80 in double-distilled H₂O), from Monday to Friday.

Statistical analyses

Statistical analyses were performed using GraphPad Prism and the R Stats package, and additional descriptions are provided in the figure legends. For the RNA-seq and ribosome profiling analysis, R/Bioconductor packages DESeq2, edgeR, and Xtail were used for statistical analysis. A false discovery rate (FDR) of <0.1 was considered

significant. Experimental raw values were depicted when possible or normalized to internal controls from at least two independent biological replicates with all data represented as means \pm SEM unless otherwise specified. When comparing data from two different groups, for example, comparisons between intact and castrate settings or a drug treatment with only two arms, Student's two-tailed t test was used to determine significance, which was set at a P value of <0.05. When we compared more than two groups, such as in the multidrug treatment study, we used analysis of variance (ANOVA) with Tukey's range test for multiple comparisons. Spearman's correlation coefficient and corresponding P value were used to measure the extent of correlation between AR and 4EBP1 in 29 LuCaP PDX models. Pearson's chi-square test was used for the correlation analysis of the GRTE. The Kaplan-Meier method with the log-rank test was used for the xenograft and PDX survival analysis. Original tumor measurements are provided in data file S2.

SUPPLEMENTARY MATERIALS

stm.sciencemag.org/cgi/content/full/11/503/eaaw4993/DC1

Materials and Methods

Fig. S1. Castration of *Pten^{L/L}* mice decreases AR, AR activity, and 4EBP1 without affecting eIF4F components.

Fig. S2. AR regulates *4ebp1* transcription but does not affect translation efficiency or degradation rates.

Fig. S3. Androgen deprivation is associated with decreased 4EBP1 expression; DHT add back decreases de novo protein synthesis.

Fig. S4. AR binds to an ARE in *4ebp1* in both normal and cancerous prostates, rendering 4EBP1 AR responsive.

Fig. S5. Castrate *Pten^{L/L}* mice develop highly aggressive, nonneuroendocrine tumors independent of PI3K or MNK1/2 activity.

Fig. S6. AR/eIF4F-sensitive mRNAs are distinct from mTOR inhibition-sensitive mRNAs.

Fig. S7. Protein but not mRNA expression of GRTE-containing proliferation regulators is responsive to changes in eIF4F activity.

Fig. S8. Decreased eIF4F complex formation by 4EBP1^M results in smaller and less aggressive tumors in castrate *Pten^{L/L};4ebp1^M* mice.

Fig. S9. Castrate *Pten^{L/L}* mice exhibit increased sensitivity to eIF4F disruption; 4EBP1 abundance is independent of AR in HSPC.

Fig. S10. 4E2RCat and 4EGI-1 disrupt eIF4F complex formation in *Pten^{L/L}* cells, AR⁺ parental, and AR⁻ AIPIC cells.

Fig. S11. AR- and eIF4F-targeted combinatorial treatments in LNCaP prostate cancer cells demonstrate antitumor activity.

Fig. S12. AR shapes the prostate cancer proteome through 4EBP1 and a druggable pro-proliferation translational regulon.

Table S1. mRNA expression of AR signature genes comparing castrate *Pten^{L/L}* ventral prostates to intact *Pten^{L/L}* ventral prostates.

Table S2. Position-weighted map of the 5'UTR GRTE.

Table S3. Primers used in this study.

Data file S1. Translationally up-regulated genes in the castrate *Pten^{L/L}* mouse.

Data file S2. Tumor measurements from in vivo experiments.

References (45–47)

REFERENCES AND NOTES

1. S. M. Dehm, D. J. Tindall, Androgen receptor structural and functional elements: Role and regulation in prostate cancer. *Mol. Endocrinol.* **21**, 2855–2863 (2007).
2. A. C. Hsieh, E. J. Small, C. J. Ryan, Androgen-response elements in hormone-refractory prostate cancer: Implications for treatment development. *Lancet Oncol.* **8**, 933–939 (2007).
3. A. Sendoel, J. G. Dunn, E. H. Rodriguez, S. Naik, N. C. Gomez, B. Hurwitz, J. Levorse, B. D. Dill, D. Schramek, H. Molina, J. S. Weissman, E. Fuchs, Translation from unconventional 5' start sites drives tumour initiation. *Nature* **541**, 494–499 (2017).
4. B. Schwanhäusser, D. Busse, N. Li, G. Dittmar, J. Schuchhardt, J. Wolf, W. Chen, M. Selbach, Global quantification of mammalian gene expression control. *Nature* **473**, 337–342 (2011).
5. R. A. J. Signer, J. A. Magee, A. Salic, S. J. Morrison, Haematopoietic stem cells require a highly regulated protein synthesis rate. *Nature* **509**, 49–54 (2014).

6. Leuprolide Study Group, Leuprolide versus diethylstilbestrol for metastatic prostate cancer. *N. Engl. J. Med.* **311**, 1281–1286 (1984).
7. P. A. Watson, V. K. Arora, C. L. Sawyers, Emerging mechanisms of resistance to androgen receptor inhibitors in prostate cancer. *Nat. Rev. Cancer* **15**, 701–711 (2015).
8. C. Tran, S. Ouk, N. J. Clegg, Y. Chen, P. A. Watson, V. Arora, J. Wongvipat, P. M. Smith-Jones, D. Yoo, A. Kwon, T. Wasieleska, D. Welsbie, C. D. Chen, C. S. Higano, T. M. Beer, D. T. Hung, H. I. Scher, M. E. Jung, C. L. Sawyers, Development of a second-generation antiandrogen for treatment of advanced prostate cancer. *Science* **324**, 787–790 (2009).
9. J. S. de Bono, C. J. Logothetis, A. Molina, K. Fizazi, S. North, L. Chu, K. N. Chi, R. J. Jones, O. B. Goodman Jr., F. Saad, J. N. Staffurth, P. Mainwaring, S. Harland, T. W. Flaig, T. E. Hutson, T. Cheng, H. Patterson, J. D. Hainsworth, C. J. Ryan, C. N. Sternberg, S. L. Ellard, A. Flechon, M. Saleh, M. Scholz, E.fstathiou, A. Zivi, D. Bianchini, Y. Loriot, N. Chieffo, T. Kheoh, C. M. Haqq, H. I. Scher, COU-AA-301 Investigators, Abiraterone and increased survival in metastatic prostate cancer. *N. Engl. J. Med.* **364**, 1995–2005 (2011).
10. H. Beltran, D. Prandi, J. M. Mosquera, M. Benelli, L. Puca, J. Cyrta, C. Marotz, E. Giannopoulou, B. V. S. K. Chakravarthi, S. Varambally, S. A. Tomlins, D. M. Nanus, S. T. Tagawa, E. M. Van Allen, O. Elemento, A. Sboner, L. A. Garraway, M. A. Rubin, F. Demichelis, Divergent clonal evolution of castration-resistant neuroendocrine prostate cancer. *Nat. Med.* **22**, 298–305 (2016).
11. E. G. Bluemn, I. M. Coleman, J. M. Lucas, R. T. Coleman, S. Hernandez-Lopez, R. Tharakan, D. Bianchi-Frias, R. F. Dumit, A. Kaipainen, A. N. Corella, Y. C. Yang, M. D. Nyquist, E. Mostaghel, A. C. Hsieh, X. Zhang, E. Corey, L. G. Brown, H. M. Nguyen, K. Pienta, M. Iltmann, M. Schweizer, L. D. True, D. Wise, P. S. Rennie, R. L. Vessella, C. Morrissey, P. S. Nelson, Androgen receptor pathway-independent prostate cancer is sustained through FGF signaling. *Cancer Cell* **32**, 474–489.e6 (2017).
12. A. C. Hsieh, H. G. Nguyen, L. Wen, M. P. Edlind, P. R. Carroll, W. Kim, D. Ruggero, Cell type-specific abundance of 4EBP1 primes prostate cancer sensitivity or resistance to PI3K pathway inhibitors. *Sci. Signal.* **8**, ra116 (2015).
13. L. Furic, L. Rong, O. Larsson, I. H. Koumaki, K. Yoshida, A. Brueschke, E. Petroulakis, N. Robichaud, M. Pollak, L. A. Gaboury, P. P. Pandolfi, F. Saad, N. Sonenberg, eIF4E phosphorylation promotes tumorigenesis and is associated with prostate cancer progression. *Proc. Natl. Acad. Sci. U.S.A.* **107**, 14134–14139 (2010).
14. X. X. Wei, A. C. Hsieh, W. Kim, T. Friedlander, A. M. Lin, M. Louttit, C. J. Ryan, A phase I study of abiraterone acetate combined with BEZ235, a dual PI3K/mTOR inhibitor, in metastatic castration resistant prostate cancer. *Oncologist* **22**, 503–e43 (2017).
15. L. Graham, K. Banda, A. Torres, B. S. Carver, Y. Chen, K. Pisano, G. Shelkey, T. Curley, H. I. Scher, T. L. Lotan, A. C. Hsieh, D. E. Rathkopf, A phase II study of the dual mTOR inhibitor MLN0128 in patients with metastatic castration resistant prostate cancer. *Invest. New Drugs* **36**, 458–467 (2018).
16. A. J. Armstrong, G. J. Netto, M. A. Rudek, S. Halabi, D. P. Wood, P. A. Creel, K. Mundy, S. L. Davis, T. Wang, R. Albadine, L. Schultz, A. W. Partin, A. Jimeno, H. Fedor, P. G. Febbo, D. J. George, R. Gurganus, A. M. De Marzo, M. A. Carducci, A pharmacodynamic study of rapamycin in men with intermediate- to high-risk localized prostate cancer. *Clin. Cancer Res.* **16**, 3057–3066 (2010).
17. S. Wang, J. Gao, Q. Lei, N. Rozenfurt, C. Pritchard, J. Jiao, G. V. Thomas, G. Li, P. Roy-Burman, P. S. Nelson, X. Liu, H. Wu, Prostate-specific deletion of the murine Pten tumor suppressor gene leads to metastatic prostate cancer. *Cancer Cell* **4**, 209–221 (2003).
18. R. J. Dowling, I. Topisirovic, T. Alain, M. Bidnost, B. D. Fonseca, E. Petroulakis, X. Wang, O. Larsson, A. Selvaraj, Y. Liu, S. C. Kozma, G. Thomas, N. Sonenberg, mTORC1-mediated cell proliferation, but not cell growth, controlled by the 4E-BPs. *Science* **328**, 1172–1176 (2010).
19. J. C. Lawrence Jr., R. T. Abraham, PHAS/4E-BPs as regulators of mRNA translation and cell proliferation. *Trends Biochem. Sci.* **22**, 345–349 (1997).
20. A. Lazaris-Karatzas, K. S. Montine, N. Sonenberg, Malignant transformation by a eukaryotic initiation factor subunit that binds to mRNA 5' cap. *Nature* **345**, 544–547 (1990).
21. A. Haghghat, N. Sonenberg, eIF4G dramatically enhances the binding of eIF4E to the mRNA 5'-cap structure. *J. Biol. Chem.* **272**, 21677–21680 (1997).
22. G. W. Rogers Jr., N. J. Richter, W. C. Merrick, Biochemical and kinetic characterization of the RNA helicase activity of eukaryotic initiation factor 4A. *J. Biol. Chem.* **274**, 12236–12244 (1999).
23. A. Pause, G. J. Belsham, A.-C. Gingras, O. Donzè, T.-A. Lin, J. C. Lawrence Jr., N. Sonenberg, Insulin-dependent stimulation of protein synthesis by phosphorylation of a regulator of 5'-cap function. *Nature* **371**, 762–767 (1994).
24. A.-C. Gingras, S. P. Gygi, B. Raught, R. D. Polakiewicz, R. T. Abraham, M. F. Hoekstra, R. Aebersold, N. Sonenberg, Regulation of 4E-BP1 phosphorylation: A novel two-step mechanism. *Genes Dev.* **13**, 1422–1437 (1999).
25. A. C. Hsieh, D. Ruggero, Targeting eukaryotic translation initiation factor 4E (eIF4E) in cancer. *Clin. Cancer Res.* **16**, 4914–4920 (2010).
26. N. T. Ingolia, S. Ghaemmaghami, J. R. S. Newman, J. S. Weissman, Genome-wide analysis in vivo of translation with nucleotide resolution using ribosome profiling. *Science* **324**, 218–223 (2009).
27. A. C. Hsieh, Y. Liu, M. P. Edlind, N. T. Ingolia, M. R. Janes, A. Sher, E. Y. Shi, C. R. Stumpf, C. Christensen, M. J. Bonham, S. Wang, P. Ren, M. Martin, K. Jessen, M. E. Feldman, J. S. Weissman, K. M. Shokat, C. Rommel, D. Ruggero, The translational landscape of mTOR signalling steers cancer initiation and metastasis. *Nature* **485**, 55–61 (2012).
28. A. Yanagiya, E. Suyama, H. Adachi, Y. V. Svitkin, P. Aza-Blanc, H. Imataka, S. Mikami, Y. Martineau, Z. A. Ronai, N. Sonenberg, Translational homeostasis via the mRNA cap-binding protein, eIF4E. *Mol. Cell* **46**, 847–858 (2012).
29. Y. Chen, P. Chi, S. Rockowitz, P. J. Iaquinta, T. Shamu, S. Shukla, D. Gao, I. Sirota, B. S. Carver, J. Wongvipat, H. I. Scher, D. Zheng, C. L. Sawyers, ETS factors reprogram the androgen receptor cistrome and prime prostate tumorigenesis in response to PTEN loss. *Nat. Med.* **19**, 1023–1029 (2013).
30. L. Boussemart, H. Malka-Mahieu, I. Girault, D. Allard, O. Hemmingsson, G. Tomasic, M. Thomas, C. Basmadjian, N. Ribeiro, F. Thuau, C. Mateus, E. Routier, N. Kamsu-Kom, S. Agoussi, A. M. Eggermont, L. Désaubry, C. Robert, S. Vagner, eIF4F is a nexus of resistance to anti-BRAF and anti-MEK cancer therapies. *Nature* **513**, 105–109 (2014).
31. A. C. Hsieh, M. Costa, O. Zollo, C. Davis, M. E. Feldman, J. R. Testa, O. Meyuhas, K. Shokat, D. Ruggero, Genetic dissection of the oncogenic mTOR pathway reveals druggable addiction to translational control via 4EBP-eIF4E. *Cancer Cell* **17**, 249–261 (2010).
32. A. Bianchini, M. Loiaro, P. Bielli, R. Busà, M. P. Paronetto, F. Loreni, R. Geremia, C. Sette, Phosphorylation of eIF4E by MNKs supports protein synthesis, cell cycle progression and proliferation in prostate cancer cells. *Carcinogenesis* **29**, 2279–2288 (2008).
33. S. L. Schuster, A. C. Hsieh, The untranslated regions of mRNAs in cancer. *Trends Cancer* **5**, 245–262 (2019).
34. C. C. Thoreen, L. Chantranupong, H. R. Keys, T. Wang, N. S. Gray, D. M. Sabatini, A unifying model for mTORC1-mediated regulation of mRNA translation. *Nature* **485**, 109–113 (2012).
35. L. Jia, Z. Zhou, H. Liang, J. Wu, P. Shi, F. Li, Z. Wang, C. Wang, W. Chen, H. Zhang, Y. Wang, R. Liu, J. Feng, C. Chen, KLF5 promotes breast cancer proliferation, migration and invasion in part by upregulating the transcription of TNFAIP2. *Oncogene* **35**, 2040–2051 (2016).
36. S. Schleich, K. Strassburger, P. C. Janiesch, T. Koledachkina, K. K. Miller, K. Haneke, Y.-S. Cheng, K. Küchler, G. Stoecklin, K. E. Duncan, A. A. Teleanu, DENR-MCT-1 promotes translation re-initiation downstream of uORFs to control tissue growth. *Nature* **512**, 208–212 (2014).
37. T. J. Chen, F. Gao, T. Yang, A. Thakur, H. Ren, Y. Li, S. Zhang, T. Wang, M. W. Chen, CDK-associated Cullin 1 promotes cell proliferation with activation of ERK1/2 in human lung cancer A549 cells. *Biochem. Biophys. Res. Commun.* **437**, 108–113 (2013).
38. R. Cencic, D. R. Hall, F. Robert, Y. Du, J. Min, L. Li, M. Qui, I. Lewis, S. Kurtkaya, R. Dingleline, H. Fu, D. Kozakov, S. Vajda, J. Pelletier, Reversing chemoresistance by small molecule inhibition of the translation initiation complex eIF4F. *Proc. Natl. Acad. Sci. U.S.A.* **108**, 1046–1051 (2011).
39. R. Cencic, M. Desforges, D. R. Hall, D. Kozakov, Y. Du, J. Min, R. Dingleline, H. Fu, S. Vajda, P. J. Talbot, J. Pelletier, Blocking eIF4E-eIF4G interaction as a strategy to impair coronavirus replication. *J. Virol.* **85**, 6381–6389 (2011).
40. N. J. Moerke, H. Aktas, H. Chen, S. Cantel, M. Y. Reibarkh, A. Fahmy, J. D. Gross, A. Degterev, J. Yuan, M. Chorev, J. A. Halperin, G. Wagner, Small-molecule inhibition of the interaction between the translation initiation factors eIF4E and eIF4G. *Cell* **128**, 257–267 (2007).
41. C. T. Wu, S. Altuwajri, W. A. Ricke, S.-P. Huang, S. Yeh, C. Zhang, Y. Niu, M.-Y. Tsai, C. Chang, Increased prostate cell proliferation and loss of cell differentiation in mice lacking prostate epithelial androgen receptor. *Proc. Natl. Acad. Sci. U.S.A.* **104**, 12679–12684 (2007).
42. V. Dubois, M. R. Laurent, F. Jardi, L. Antonio, K. Lemaire, L. Goyvaerts, L. Deldicque, G. Carmeliet, B. Decallonne, D. Vanderschueren, F. Claessens, Androgen deficiency exacerbates high-fat diet-induced metabolic alterations in male mice. *Endocrinology* **157**, 648–665 (2016).
43. O. Le Bacquer, E. Petroulakis, S. Paglialunga, F. Poulin, D. Richard, K. Cianflone, N. Sonenberg, Elevated sensitivity to diet-induced obesity and insulin resistance in mice lacking 4E-BP1 and 4E-BP2. *J. Clin. Invest.* **117**, 387–396 (2007).
44. S.-Y. Tsai, A. A. Rodriguez, S. G. Dastidar, E. Del Greco, K. L. Carr, J. M. Sitzmann, E. C. Academia, C. M. Viray, L. L. Martinez, B. S. Kaplowitz, T. D. Ashe, A. R. La Spada, B. K. Kennedy, Increased 4E-BP1 expression protects against diet-induced obesity and insulin resistance in male mice. *Cell Rep.* **16**, 1903–1914 (2016).
45. T. L. Bailey, C. Elkan, Fitting a mixture model by expectation maximization to discover motifs in biopolymers. *Proc. Int. Conf. Intell. Syst. Mol. Biol.* **2**, 28–36 (1994).
46. C. E. Grant, T. L. Bailey, W. S. Noble, FIMO: Scanning for occurrences of a given motif. *Bioinformatics* **27**, 1017–1018 (2011).

47. Z. Xiao, Q. Zou, Y. Liu, X. Yang, Genome-wide assessment of differential translations with ribosome profiling data. *Nat. Commun.* **7**, 11194 (2016).

Acknowledgments: We are grateful to the patients who participated in this study and their families. We thank members of the A.C.H. laboratory for helpful advice. We thank J. M. Shen for editing the manuscript. We thank A. Geballe, A. Subramaniam, C. Ghajar, and C. Bellodi for critical discussion of the paper. We thank L. Xin for providing ChIP-seq and RNA-seq data from wild-type murine prostate luminal epithelial cells. We thank S. Kugel for providing Riptag2 neuroendocrine cells. **Funding:** This work was supported by NIH award 1R37CA230617, the Pacific Northwest Prostate Cancer SPORE (P50CA097186, P01CA163227, and CA182503-01A1), the CDMRP (W81XWH-17-1-0415), and the Shared Resources of FHCRC/UW Cancer Consortium (P30 CA015704). A.C.H. is a V Foundation Scholar and is funded by a NextGen Grant for Transformative Cancer Research from the American Association for Cancer Research (AACR) and a Burroughs Wellcome Fund Career Award for Medical Scientists. K.B. is a recipient of an American Society of Clinical Oncology Endowed Young Investigator Award in memory of S. Gordon, a National Cancer Institute training grant (T32CA009515), and a Pilot and Feasibility Studies Program grant funded by the Cooperative Center for Excellence in Hematology (U54 DK106829). Y. Lim received funding through a Department of Defense Prostate Cancer Research Program Postdoctoral Training Award (PC150946) and the AACR. A.C.H., Y.C., and B.S.C. are funded by a Movember-Prostate Cancer Foundation Challenge Award. **Author contributions:** A.C.H. conceived the project; Y. Liu, J.L.H., K.B., and A.Z.G., performed mouse experiments; Y. Liu, J.L.H., A.A.G., L.W., W.R.H., and K.B. conducted molecular and cell biology experiments; Y. Lim conducted the ribosome profiling experiment; S.J. conducted the in vitro proximity ligation assay; R.G.T., Y.C.Y., I.M.C., and P.S.N. assisted with the RNA-seq experiment; Y.C. conducted the ChIP-seq analysis;

E.Y.C. and S.B. assisted with shRNA experiments; B.S.C. assisted with enzalutamide experiments; A.A.G. conducted the 5'UTR studies; S.A. conducted computational analysis; T.U. and S.R.P. assisted with ARE experiments; S.P.S.P. conducted blinded pathology evaluation; E.C. and C.M. provided biospecimens and AR staining in the human studies; A.C.H. wrote the manuscript with input from Y. Liu, J.L.H., K.B., Y. Lim, S.J., and A.A.G.; all authors reviewed and edited the manuscript. **Competing interests:** A.C.H. receives research funding from EFFECTOR Inc. P.S.N. has consulted for Janssen and Astellas Pharma Inc. All other authors declare that they have no competing interests. **Data and materials availability:** Raw RNA-seq and ribosome profiling sequencing data can be accessed at Sequence Read Archive (SRP151005 and SRP151006) and NCBI Gene Expression Omnibus (GSE116081 and GSE116082). Raw ChIP-seq data from *Pten^{fl/fl}* prostates were obtained from Gene Expression Omnibus (GSE47119). All other data associated with this study are present in the paper or the Supplementary Materials.

Submitted 1 January 2019

Resubmitted 23 April 2019

Accepted 24 June 2019

Published 31 July 2019

10.1126/scitranslmed.aaw4993

Citation: Y. Liu, J. L. Horn, K. Banda, A. Z. Goodman, Y. Lim, S. Jana, S. Arora, A. A. Germanos, L. Wen, W. R. Hardin, Y. C. Yang, I. M. Coleman, R. G. Tharakan, E. Y. Cai, T. Uo, S. P. S. Pillai, E. Corey, C. Morrissey, Y. Chen, B. S. Carver, S. R. Plymate, S. Beronja, P. S. Nelson, A. C. Hsieh, The androgen receptor regulates a druggable translational regulon in advanced prostate cancer. *Sci. Transl. Med.* **11**, eaaw4993 (2019).

Science Translational Medicine

The androgen receptor regulates a druggable translational regulon in advanced prostate cancer

Yuzhen Liu, Jessie L. Horn, Kalyan Banda, Asha Z. Goodman, Yiting Lim, Sujata Jana, Sonali Arora, Alexandre A. Germanos, Lexiaochuan Wen, William R. Hardin, Yu C. Yang, Ilsa M. Coleman, Robin G. Tharakan, Elise Y. Cai, Takuma Uo, Smitha P. S. Pillai, Eva Corey, Colm Morrissey, Yu Chen, Brett S. Carver, Stephen R. Plymate, Slobodan Beronja, Peter S. Nelson and Andrew C. Hsieh

Sci Transl Med 11, eaaw4993.
DOI: 10.1126/scitranslmed.aaw4993

Driving out translation to treat cancer

The androgen receptor is a well-known driver of prostate cancer and a common therapeutic target in this disease. Now, Liu *et al.* have identified an unexpected link between the androgen receptor and regulation of mRNA translation. The authors determined that the androgen receptor has a suppressive effect on protein synthesis, whereas the loss of this receptor is associated with increased initiation of translation, facilitating tumor cell proliferation. This observation helps explain the rapid growth of late-stage androgen receptor-deficient prostate cancer and provides a therapeutic opportunity through inhibition of a translation initiation complex, which the authors demonstrate in mouse models.

ARTICLE TOOLS	http://stm.sciencemag.org/content/11/503/eaaw4993
SUPPLEMENTARY MATERIALS	http://stm.sciencemag.org/content/suppl/2019/07/29/11.503.eaaw4993.DC1
RELATED CONTENT	http://stm.sciencemag.org/content/scitransmed/7/269/269ra2.full http://stm.sciencemag.org/content/scitransmed/8/333/333ra47.full http://stm.sciencemag.org/content/scitransmed/11/498/eaaw4636.full http://stm.sciencemag.org/content/scitransmed/10/439/eaar2036.full
REFERENCES	This article cites 47 articles, 13 of which you can access for free http://stm.sciencemag.org/content/11/503/eaaw4993#BIBL
PERMISSIONS	http://www.sciencemag.org/help/reprints-and-permissions

Use of this article is subject to the [Terms of Service](#)

Science Translational Medicine (ISSN 1946-6242) is published by the American Association for the Advancement of Science, 1200 New York Avenue NW, Washington, DC 20005. 2017 © The Authors, some rights reserved; exclusive licensee American Association for the Advancement of Science. No claim to original U.S. Government Works. The title *Science Translational Medicine* is a registered trademark of AAAS.